



Contents lists available at ScienceDirect

Chemical Physics Letters

journal homepage: www.elsevier.com/locate/cplett

On the origin of IR spectral changes upon protein folding

Isabella Daidone^{a,*}, Massimiliano Aschi^a, Laura Zanetti-Polzi^b, Alfredo Di Nola^b, Andrea Amadei^{c,*}

^aDipartimento di Chimica Ingegneria, Chimica e Materiali, University of L'Aquila, via Vetoio (Coppito 1), 67010 Coppito (AQ), Italy

^bDipartimento di Chimica, University of Rome 'La Sapienza', P.le Aldo Moro 5, 00185 Rome, Italy

^cDipartimento di Scienze e Tecnologie Chimiche, University of Rome 'Tor Vergata', via della Ricerca Scientifica 1, 00133 Rome, Italy

ARTICLE INFO

Article history:

Received 11 December 2009

In final form 9 February 2010

Available online xxx

ABSTRACT

The unfolded- and folded-state infrared (IR) spectra of peptides studied to date show a common pattern, *i.e.*, the amide I peak of the unfolded state is typically shifted toward higher frequencies with respect to the folded peak. Here, we study by means of a theoretical–computational method, the Perturbed Matrix Method (PMM), the IR spectra in the amide I region of two β -hairpin peptides. The computed spectra are in good agreement with the experimental ones, thus providing an explanation of the physical origin underlying the differences of the unfolded- and folded-state spectra.

© 2010 Elsevier B.V. All rights reserved.

1. Introduction

Infrared (IR) absorption spectra of amide modes (particularly of the amide I mode, mostly corresponding to the peptide-group C=O stretching) have long provided a tool for determining the secondary structure of peptides and proteins [1–3]. Theoretical and computational analyses have aided in providing the rather well-established structure–frequency correlations [4–19]. A number of these studies [2,8,9,11–14,18,19] has suggested that the amide I absorption patterns of folded structural elements, such as the β -sheet, can be explained by the symmetry of the given structure and points to a crucial role played by excitonic coupling of the amide I oscillators. On the contrary, the physical origin of the spectroscopic behaviours of unfolded states is much less understood, despite differences in the amide I bands of folded and unfolded states having become a crucial spectral feature to follow protein and peptide folding kinetics and kinetics in time-resolved and temperature dependent IR spectroscopies [20–24].

Interestingly, the unfolded- and folded-state spectra of the peptides studied to date by IR spectroscopy, both α -helical [20,21] and β -hairpins [22–24], the basic secondary structural elements of proteins, show a common pattern regardless of the specific secondary structure, *i.e.*, the amide I peak of the unfolded state is typically shifted toward higher frequencies with respect to the folded peak (which is commonly centered at around 1630–1640 cm^{-1}). What is the origin of such a shift? Are there perturbing effects other than the usually mentioned excitonic coupling, playing an important role? These are crucial, still open, questions that we address in the present work.

In this Letter, the amide I band of two β -hairpin peptides, a 15-residue designed peptide termed peptide 1 and a 10-mer cyclic analog of Gramicidin S, GS10, are evaluated using a theoretical–computational approach based on the Perturbed Matrix Method (PMM), a mixed quantum mechanics/molecular dynamics (QM/MD) method [25–28] whose main aim is to keep the configurational complexity of the system (peptide + solvent molecules) with a proper treatment of the quantum degrees of freedom of a portion of the system to be explicitly treated at electronic level (the backbone peptide group). Such a method has been already successfully applied to reproduce the IR spectrum of aqueous carbon monoxide [25], of carbon monoxide within Myoglobin [26] and of liquid water [28]. The good agreement observed, here, between the theoretical and experimental spectra of the two peptides shows the basic correctness of the calculations. Therefore, the conclusions on the contribution of individual, or subsets of, peptide groups to the spectra are considered to be meaningful, allowing the structure–spectrum correlations in unfolded–folded amide I difference spectra to be understood at atomic detail.

2. Theory and methods

In PMM calculations [25–28], similarly to other QM/MM procedures [29], it is essential to pre-define a portion of the system to be treated at electronic level, hereafter termed as quantum center (QC), with the rest of the system described at a classical atomistic level exerting an electrostatic perturbation on the QC electronic states. An orthonormal set of unperturbed electronic Hamiltonian (\tilde{H}^0) eigenfunctions (Φ_k^0) are initially evaluated on the QC structure of interest which is typically the ground state equilibrium geometry (note that such an energy minimised structure is virtually identical for the perturbed and unperturbed ground states). Indicating

* Corresponding authors. Fax: +39 06 7259 4328 (A. Amadei).

E-mail addresses: daidone@caspur.it (I. Daidone), andrea.amadei@uniroma2.it (A. Amadei).

with \mathcal{V} and \mathbf{E} the perturbing electric potential and field, respectively, exerted by the environment on the QC (typically obtained by the environment atomic charge distribution and evaluated in the QC center of mass) we may, then, construct for each QC-environment configuration (as generated by explicit solvent MD simulation) the perturbed electronic Hamiltonian matrix (\tilde{H}) as follows:

$$\tilde{H} \cong \tilde{H}^0 + \tilde{I}q_T\mathcal{V} + \tilde{Z}_1 + \Delta V\tilde{I} \quad (1)$$

$$\left[\tilde{Z}_1\right]_{kk'} = -\mathbf{E} \cdot \left\langle \Phi_k^0 | \hat{\mu} | \Phi_{k'}^0 \right\rangle \quad (2)$$

where q_T and $\hat{\mu}$ are the QC total charge and dipole operator, respectively, ΔV approximates all the higher order terms as a simple short range potential, \tilde{I} is the identity matrix and the angled brackets indicate integration over the electronic coordinates. The diagonalisation of \tilde{H} provides a set of eigenvectors and eigenvalues representing the QC perturbed electronic eigenstates and energies.

For the more specific task of determining perturbed vibrational states, the following procedure is used. Firstly, the unperturbed QC mass-weighted Hessian eigenvectors are defined by standard QM calculations on the isolated quantum center. Then, once the mode of interest is selected, a number of QC configurations along the mode coordinate, q , are generated. For each of these QC configurations an orthonormal set of unperturbed electronic eigenfunctions can be obtained by standard QM procedures and, using Eqs. (1) and (2), a number of perturbed electronic Hamiltonian eigenstates and eigenvalues may be evaluated at each MD frame. Subsequently, the perturbed electronic ground state energy, ϵ_0 (i.e., the ground state eigenvalue of the matrix \tilde{H}), along the mode coordinate q can be expressed at each time frame as follows:

$$\epsilon_0(q, t) \cong \epsilon_0'(q, t) + q_T\mathcal{V}(t) + \Delta V(q, t) \quad (3)$$

with ϵ_0' the ground state eigenvalue of the matrix $\tilde{H}^0 + \tilde{Z}_1$ (Eqs. (1) and (2)). Finally, the perturbed harmonic frequency, $\omega/2\pi$, is evaluated at each time frame via a polynomial fit of such an energy curve, providing the second order energy derivative at the minimum position (note that ΔV along the mode coordinate can be disregarded as this higher order term provides weak effects on the energy derivatives which are averaged out when the frequency spectrum is calculated).

The basic approximation of the method is that for typical quantum vibrational degrees of freedom the environment perturbation does not significantly alter the vibrational modes (i.e., the mass-weighted QC Hessian eigenvectors) but only the related eigenvalues (ω^2). Such an assumption provides a good approximation when we consider a vibrational mode which, under the perturbation, remains largely uncoupled from the other QC modes as well as from the vibrational modes of the QC atomic-molecular environment. This approximation implies that the possible amide I modes excitonic effect is disregarded. Although many studies [31,30] suggest an important role for exciton coupling in polypeptides and inclusion of such a coupling within the PMM framework is possible, as described in details in a recent paper [27], in this work we neglect such interactions. In fact, the model systems analysed in the present work are two small β -hairpin peptides (i.e., with a limited sheet structure) for which the typical excitonic spectroscopic signature, i.e., the weaker band at about 1680–1690 cm^{-1} , is not evident in the experimental spectra. Therefore, in this Letter we focus on the less investigated effect of the environment ground-state perturbation on the quantum states of each peptide group, i.e., the coupling between each localised vibrational mode and the environment atomic motions. Nevertheless, in a further paper we will specifically address the effect of excitonic coupling, investigating its role in peptide folding-unfolding IR signal variations.

As a model of the peptide group, i.e., the quantum center to be explicitly treated at electronic level, trans-N-methylacetamide

(trans-NMA) was chosen. As a benchmark, the PMM/MD procedure described above has been initially applied to reconstruct the amide I mode of trans-NMA in D_2O solution (see below). Subsequently, the same protocol has been adopted also for evaluating perturbed amide I frequencies for the peptide groups (residues) belonging to the N -residues β -hairpin peptides in D_2O solution. Trans-NMA fitted to the peptide group of each residue was used as the corresponding QC and hence its (unperturbed) mass-weighted Hessian eigenvectors provide the vibrational modes of each peptide group. The sidechain of the considered peptide group, the $N - 1$ residues and the solvent define the perturbing environment at each configuration generated by MD simulation and the distribution of the oscillators perturbed-frequencies make up the total amide I band.

2.1. Unperturbed quantum chemical calculations

Quantum chemical calculations were carried out on the isolated trans-NMA molecule at the Time Dependent Density Functional Theory (TD-DFT) level with the 6-31+G (d) basis set. This level of theory was selected because it represents a good compromise between computational costs and accuracy. The mass-weighted Hessian matrix was calculated on the optimised geometry at the B3LYP/6-31+G (d) level of theory and subsequently diagonalised for obtaining the unperturbed eigenvectors and related eigenvalues. The eigenvector corresponding in vacuo to the amide I mode was, then, used to generate a grid of points (i.e., configurations) as follows: a step of 0.05 a.u. was adopted and the number of points was set to span an energy range of 20 kJ/mol (in the present case 31 points). For each point, six unperturbed electronic states were then evaluated at the same level of theory providing the basis set for the PMM calculations, i.e., the Φ_k^0 eigenfunctions in Eqs. (1) and (2).

2.2. Molecular dynamics simulations

A series of 50 ns-long atomistic MD simulations of peptide 1 and GS10 were performed in explicit solvent. For each peptide, six independent simulations were performed to generate the ensemble of structures to be used to compute the total amide I peak. Three of these simulations, representing the unfolded state and used to compute the unfolded-state amide I peak, were started from unfolded structures and the other three, representing the folded state and used to compute the folded-state amide I peak, from folded structures. The three starting structures for the unfolded-state simulations were extracted randomly from a simulation of 10 ns that was started from a fully extended configuration, for peptide 1, and from a high-temperature-generated structure for the cyclic GS10 peptide; the three starting structures for the folded-state simulations were taken from a simulation of 10 ns that was started from the NMR structure. The MD simulations were performed with the program GROMACS [32] and the GROMOS96 force field [33] was used for the peptide. The solvent used was D_2O , to reproduce the experimental conditions, and was modelled using the deuterated spc water model [34]. Each of the starting configurations was placed in a dodecahedral water box large enough to contain the peptide and at least 1.0 nm of solvent on all sides at a water density of 55.32 mol/l. Periodic boundary conditions were used and the long range electrostatic interactions were treated with the Particle Mesh Ewald method [35]. Coordinates were saved at every 1 ps. Simulations were performed in the NVT ensemble with the isokinetic temperature coupling [36] to keeping the temperature constant at 300 K. Three positive (Na^+) and two negative (Cl^-) counter ions for peptide 1 and GS10, respectively, were added by replacing the corresponding number of water molecules so as to achieve a neutral simulation box. A 20 ns-long atomistic MD simulation of trans-NMA in aque-

ous solution was performed in explicit solvent (deuterated spc water model [34]) using the same conditions and simulation protocol described above. For the trans-NMA equilibrium structure, that was kept fixed during the simulation, the DFT-based optimisation as described above was used. Atomic charges were calculated using standard fitting procedures [37] on the optimised geometry at the B3LYP/6-31+G (d) level of theory.

2.3. Infrared spectra of trans-NMA

The amide I experimental vibrational frequency of the isolated trans-NMA ranges from 1707 cm^{-1} (in an argon matrix at 20 K [38]) to $1714\text{--}1731\text{ cm}^{-1}$ (in the gas phase at $\approx 100\text{ K}$ [39]) depending on the experimental conditions. The computed unperturbed amide I frequency, evaluated here using standard geometry optimisations and frequency calculations at the harmonic approximation, is 1754 cm^{-1} , 47 cm^{-1} higher than the experimental one (we take as the reference experimental value the one recorded in the argon matrix at 20 K [38]). This shift is rather common for this kind of calculations [38,40] and is usually attributed to various slight inaccuracies of the quantum calculations including the harmonic approximation, as indicated by a recent work providing for the amide I mode of trans-NMA a $\approx 30\text{ cm}^{-1}$ anharmonic correction [41].

The experimental IR spectrum of trans-NMA in the amide I region in D_2O solvent at room temperature is presented in Fig. 1 (the data are taken from Ref. [42]). The maximum of the amide I peak in solution is at about $1622\text{--}1623\text{ cm}^{-1}$, i.e., downshifted by $\approx 80\text{--}85\text{ cm}^{-1}$ with respect to the frequency of the isolated trans-NMA [4,39] (unperturbed frequency), with a full width at half maximum (fwhm) of $\approx 30\text{ cm}^{-1}$. The amide I band of trans-NMA in D_2O solution, computed using the PMM/MD procedure, provides a spectrum with the maximum at 1698 cm^{-1} corresponding to a downshift of 56 cm^{-1} with respect to the unperturbed frequency and hence reproducing most of the large negative frequency shift experimentally observed. Further, the spectrum shape and width is very well reproduced by PMM/MD calculations (fwhm = 30 cm^{-1}) as clearly shown in Fig. 1. It is worth noting that the missing $25\text{--}30\text{ cm}^{-1}$ of the PMM/MD-derived shift with respect to the experimental one are due to a combination of higher order effects possibly including the slight inaccuracies of the calculated dipoles involved in the definition of the \tilde{Z}_1 matrix (Eqs. (1) and (2)) and the fact that we disregard any excitonic coupling and/or anharmonic behaviour.

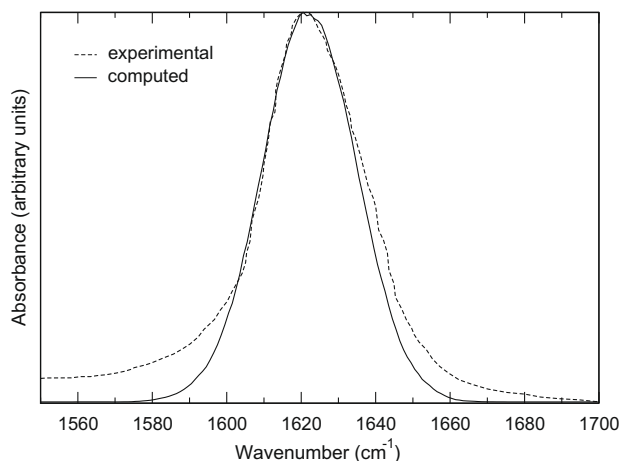


Fig. 1. Comparison of the computed and experimental [42] infrared spectra in the amide I region of trans-NMA in D_2O solution. For the sake of comparison, the computed frequencies have been uniformly shifted to lower frequencies by 76 cm^{-1} in order to align the computed to the experimental peak centered at 1622 cm^{-1} .

3. Results and discussion

Here, the amide I band of two β -hairpin peptides, a 15-residue designed peptide termed peptide 1 and a 10-mer cyclic analog of Gramicidin S, GS10 (see Fig. 2), are evaluated using the PMM/MD procedure described in the Section 2 section. The experimentally-derived [22,23] and computed amide I band of peptide 1 in D_2O

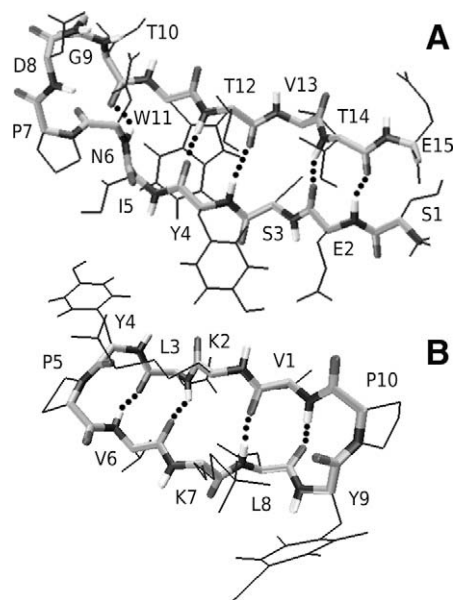


Fig. 2. NMR-derived β -hairpin structures of peptide 1 [22] (SESYPNGTWTVTE) (A) and GS10 [23] (VKLYPVKLYP) (B). The peculiar feature of these two peptides is that they show an opposite pattern of the aminoacids of the β -sheet with the hydrogen-bonded C=O groups pointing inwards (in) or with the C=O groups pointing towards the solvent (out), i.e., for GS10 the 'in' residues are hydrophobic and the 'out' residues are hydrophilic, while for peptide 1 the 'in' residues are hydrophilic and the 'out' residues are mainly hydrophobic.

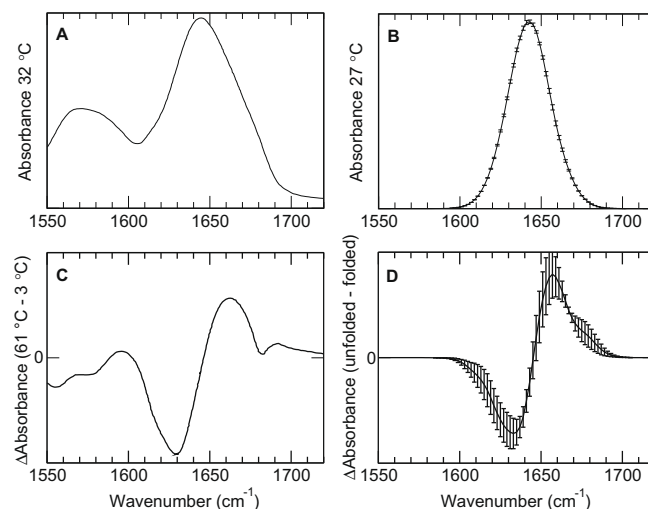


Fig. 3. Experimental [22] (A) and computed (B) infrared spectra in the amide I region of peptide 1 in D_2O solution. The experimental difference spectrum (C) was generated by subtracting the spectrum collected at $3.0\text{ }^\circ\text{C}$ from the one collected at $61.0\text{ }^\circ\text{C}$. The computed difference spectrum (D) was generated by subtracting the spectrum of the folded state from the spectrum of the unfolded state. For the sake of comparison, the computed frequencies (panels B and D) have been uniformly shifted to lower frequencies by 73 cm^{-1} in order to align the computed amide I peak to the experimental maximum at 1644 cm^{-1} . The absorbances are given in arbitrary units. The error bars correspond to a standard error of the corresponding property estimated over three independent sets of trajectories.

at room temperature are shown in Fig. 3A and B, respectively (the data for GS10, being very similar, are not shown). The computed peak-maximum frequency is upshifted by 73 cm^{-1} with respect to the experimental one, which is at 1644 cm^{-1} . This shift is largely determined by the slight inaccuracies of the QM-based calculations, as discussed in the Theory and Methods section. However, PMM/MD calculations accurately reproduce the frequency shift of peptide 1 and trans-NMA maxima (19 cm^{-1} versus the experimental 22 cm^{-1}) and provide most of the experimentally observed width of peptide 1 principal absorption peak.

In the experiments, spectra at different temperatures are collected to monitor folded and unfolded populations (within the usual assumption that the higher the temperature, the higher the unfolded population). As the temperature decreases (*i.e.*, folded state population increases), the amide I band shifts to lower frequency and therefore the unfolded–folded absorption difference spectrum (corresponding to the difference of the spectra at the extreme temperatures) shows a negative signal at $\approx 1630\text{ cm}^{-1}$ and a positive signal at $\approx 1665\text{ cm}^{-1}$, crossing zero at $\approx 1645\text{ cm}^{-1}$ (see Fig. 3C).

To shed light into the structure/spectrum correlations, the spectra of the folded and unfolded states are here calculated by applying the PMM/MD procedure to the folded and unfolded state ensembles, respectively, as generated by the MD simulations of the peptides (see Section 2 section). The calculated difference spectrum (unfolded–folded) of peptide 1 is presented in Fig. 3D and is in very good agreement with the experimental one, showing the characteristic negative–positive signature (the data for GS10, being very similar, are not shown). The good quantitative reproduction of the peptides IR signals justifies the use of the model employed to

investigate further the origin of the folding–unfolding spectral features.

One useful characteristic of our approach is that the amide I signal arising from any desired peptide group of the polypeptide chain may be isolated. In Fig. 4A the contributions from each peptide group (aminoacid) to the difference spectrum are shown together, along with the total signal. Interestingly, it can be seen that part of the residues shows the negative–positive signal, while others show the opposite trend. The questions arise to which is the origin of the two different trends for different aminoacids and to why the total IR difference spectrum of the peptides appeared to date [20–24], which are both α -helices and β -hairpins, shows the negative–positive signature. In what follows we investigate the role played by two factors: the position of the residue in the folded β -sheet, *i.e.*, with the hydrogen-bonded C=O groups pointing inwards (in) or with the C=O groups pointing towards the solvent (out), and the nature of the side chain, *i.e.*, hydrophobic (phobic) or hydrophilic (philic).

The contributions to the difference spectrum arising from these different factors were evaluated by summing up the signals of the individual residues belonging to the given category. These are shown in Fig. 4B and C. It can be observed that the role played by the position in the folded structure is not unique in the two pep-

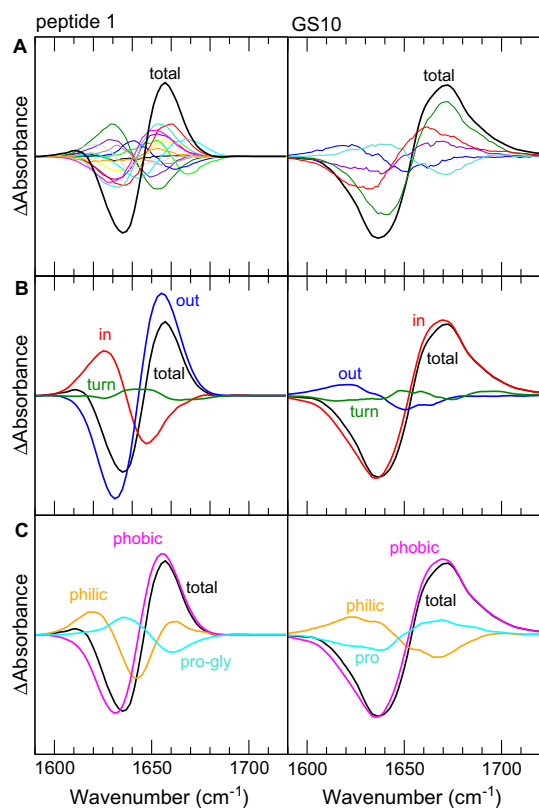


Fig. 4. Contribution of the single peptide groups to the computed unfolded–folded amide I difference spectrum for peptide 1 (left) and GS10 (right). (A) All the peptide groups are shown separately. (B) The signals arising from 'in', 'out' and 'turn' peptide groups are grouped into three separated groups. (C) The signals from 'phobic', 'philic' and aminoacids not included into any category (pro and gly) are grouped into three separated groups. The absorbances are given in arbitrary units.

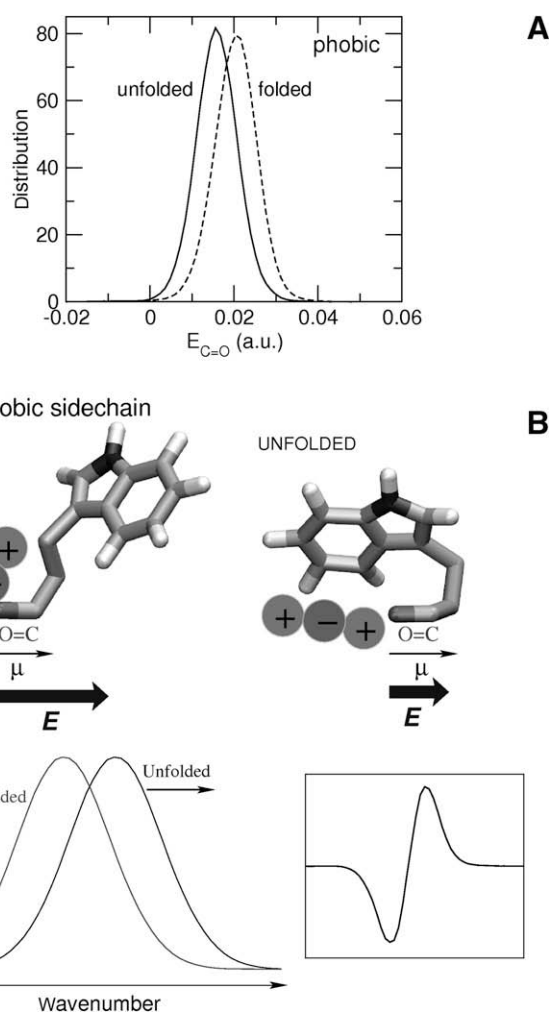


Fig. 5. Effect of the hydrophobic sidechains on the amide I band. (A) Component of the electric field along the C=O dipole of the peptide group, $E_{C=O}$, for a representative hydrophobic residue in the unfolded and folded states. (B) Scheme summarising the effect of the hydrophobic sidechain on the amide I mode vibrational frequency of the peptide group, to which the sidechain is attached, in the folded and unfolded states.

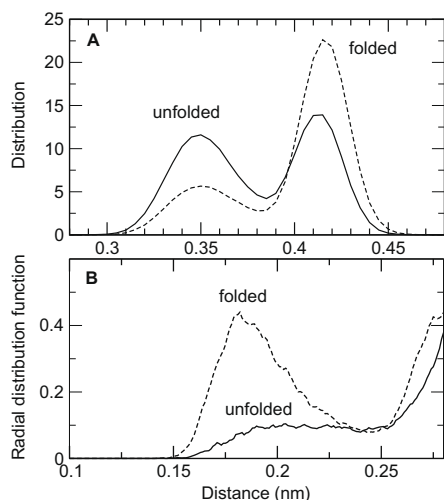


Fig. 6. Distributions of the sidechain-carbonyl distance (distance between the corresponding centers of mass) (A) and radial distribution functions of the polar atoms around the peptide carbonyl group (B) for the unfolded (solid line) and folded (dashed line) states of a representative hydrophobic residue. It can be noted that in the unfolded state the population at shorter distances is increased, thus implying that the sidechain is closer to its peptide group in the unfolded state than in the folded one. This provides a decreased density of the polar atoms close to the carbonyl group in the unfolded state.

tides, *i.e.*, for peptide 1 the 'in' residues show a positive–negative signal and the 'out' residues a negative–positive signal, while the opposite is true in the GS10 peptide. Instead, the nature of the side chain, regardless of its position in the folded structure, shows the same trend in both peptides, *i.e.*, all residues with a hydrophobic sidechain show a negative–positive signal giving rise to a pronounced negative–positive contribution to the total signal, while residues with a hydrophilic sidechain show both trends (*e.g.*, the red curves in Fig. 4A) giving rise to a weak positive–negative overall contribution (Fig. 4C). Hence, the global negative–positive spectroscopic feature arises from the overcompensating contribution of the hydrophobic sidechains.

Why do the hydrophobic sidechains provide a negative–positive signal in the unfolded–folded difference spectrum, *i.e.*, why is the unfolded amide I peak shifted to higher frequencies with respect to the folded band? To answer this question, we studied the effect of the electric field, E , exerted by the environment on the different vibrating C=O dipoles. The component of the electric field along the vibrating C=O dipole, $E_{C=O}$, for a representative hydrophobic aminoacid in the unfolded and folded states is reported in Fig. 5A. It can be seen that for the hydrophobic sidechains $E_{C=O}$ is lower in the unfolded state, giving rise to the observed shift to higher frequencies of the amide I band with respect to the folded state (negative–positive signal in the unfolded–folded difference spectrum) (see scheme in Fig. 5B).

Such electric field variations mainly arise from the fact that the sidechain of the hydrophobic aminoacids of the studied peptides is on average closer to its own and/or neighbouring peptide group in the unfolded state with respect to the folded configurations (see Fig. 6A). In the unfolded configurations, the hydrophobic sidechains provide a less polar environment to the vibrating amide I mode (mainly C=O stretching) – Fig. 5B, as a consequence of the more compact backbone–sidechain conformation resulting in a decreased density of the environment polar atoms surrounding the peptide group carbonyl (see Fig. 6B).

Therefore, such decreased local electrostatic interactions lead to a shift of the unfolded peak toward higher frequencies, *i.e.*, towards the amide I band of the isolated peptide group (which is at around 1700–1750 cm^{-1} – see Section 2). The global negative–positive

signal in the unfolded–folded amide I difference spectrum, being made up of all the peptide groups, is hence dominated by the effect of the hydrophobic sidechains (Fig. 5B).

4. Conclusions

The good quantitative reproduction of the experimental IR spectral behaviour of the studied peptides, as obtained by the PMM/MD procedure used in this Letter disregarding any excitonic coupling, indicates that the main features of the unfolded–folded difference spectrum (at least for the studied hairpins) may be reproduced by the amide I mode–environment interactions, thus pointing to an essential role played by the environment perturbation on each localised vibrational mode. These results show that a physically coherent procedure, not involving the use of empirical, adjustable parameters, may provide an efficient tool to characterise and interpret IR spectral differences upon folding of peptides and, possibly, proteins in solution in terms of their atomistic behaviour. One possible outlook is a further development of the method to other effects, such as anharmonic correction and excitonic coupling, in order to study and interpret in more details polypeptide IR signals and to approach to 2D IR spectra which are recent tools used to probe structures and dynamics in complex systems [3,19,24,30].

Acknowledgements

This work was supported by the Italian FIRB RBIN04PWNC_001 'Structure, function, dynamics and folding of proteins' funded by MIUR. We also acknowledge the University of Rome 'La Sapienza' for financial support with the project 'Morfogenesi Molecolare: un approccio multidisciplinare per lo studio del folding e misfolding delle proteine' and CASPUR (Consorzio interuniversitario per le Applicazioni di Supercalcolo Per Università e Ricerca) for the use of its computational facilities.

References

- [1] M. Jackson, H.H. Mantsch, *Crit. Rev. Biochem. Mol. Biol.* 30 (1995) 95.
- [2] A. Barth, C. Zscherp, *Q. Rev. Biophys.* 35 (2002) 369.
- [3] C. Fang, A. Senes, L. Cristian, W.F. DeGrado, R.M. Hochstrasser, *Proc. Natl. Acad. Sci. USA* 103 (2007) 16740.
- [4] K. Kwac, M. Cho, *J. Chem. Phys.* 119 (2003) 2247.
- [5] J.R. Schmidt, S.A. Corcelli, J.L. Skinner, *J. Chem. Phys.* 121 (2004) 8887.
- [6] M.P. Gaigeot, R. Vuilleumier, M. Sprik, D. Borgis, *J. Chem. Theor. Comput.* 1 (2005) 772.
- [7] R.D. Gorbunov, P.H. Nguyen, M. Kobus, G. Stock, *J. Chem. Phys.* 126 (2007) 054509.
- [8] S. Krimm, J. Bandekar, *Adv. Protein Chem.* 38 (1986) 181.
- [9] H. Torii, M. Tasumi, *J. Chem. Phys.* 96 (1992) 3379.
- [10] S.H. Lee, S. Krimm, *Biopolymers* 46 (1998) 283.
- [11] A. Moran, S. Mukamel, *Proc. Natl. Acad. Sci. USA* 101 (2004) 506.
- [12] J.W. Brauner, C.R. Flach, R. Mendelsohn, *J. Am. Chem. Soc.* 127 (2005) 100.
- [13] S. Yang, M. Cho, *J. Chem. Phys.* 123 (2005). 134503.
- [14] P. Bour, T.A. Keiderling, *J. Phys. Chem. B* 109 (2005) 23687.
- [15] A.W. Smith, A. Tokmakoff, *J. Chem. Phys.* 126 (2007). 045109.
- [16] S. Ham, S. Cha, J.H. Choi, M. Cho, Amide I modes of tripeptides: Hessian matrix reconstruction and isotope effects, *J. Chem. Phys.* 119 (2003). 1451.
- [17] S. Hahn, S. Ham, M. Cho, *J. Phys. Chem. B* 109 (2005) 11789.
- [18] J.H. Choi, H. Lee, K.K. Lee, S. Hahn, M. Cho, *J. Chem. Phys.* 126 (2007). 045102.
- [19] T. Hayashi, S. Mukamel, *J. Phys. Chem. B* 111 (2007) 11032.
- [20] C. Huang, Z. Getahun, Y. Zhu, J. Klemke, W. DeGrado, F. Gai, *Proc. Natl. Acad. Sci. USA* 99 (2002) 2788.
- [21] J.A. Ihalainen et al., *Proc. Natl. Acad. Sci. USA* 104 (2007) 5383.
- [22] Y. Xu, R. Oyola, F. Gai, *J. Am. Chem. Soc.* 125 (2003) 15388.
- [23] S.J. Maness, S. Franzena, A.C. Gibbs, T.P. Causgrove, R.B. Dyer, *Biophys. J.* 84 (2003) 3874.
- [24] A.W. Smith, A. Tokmakoff, *Angew. Chem. Int. Ed. Engl.* 46 (2007) 7984.
- [25] A. Amadei, F. Marinelli, M. D'Abramo, M. D'Alessandro, M. Anselmi, A. Di Nola, M. Aschi, *J. Chem. Phys.* 122 (2005) 124506.
- [26] M. Anselmi, M. Aschi, A. Di Nola, A. Amadei, *Biophys. J.* 92 (2007) 3442.
- [27] A. Amadei, M. D'Alessandro, M. D'Abramo, M. Aschi, *J. Chem. Phys.* 130 (2009) 08410.
- [28] M. Aschi, A. Amadei, *IJLSS*, in press.

- [29] J. Gao, D.G. Truhlar, *Ann. Rev. Phys. Chem.* 53 (2002) 467.
- [30] L.P. DeFlores, Z. Ganim, R.A. Nicodemus, A. Tokmakoff, *J. Am. Chem. Soc.* 131 (2009) 3385.
- [31] Z. Ganim, H.S. Chung, A.W. Smith, L.P. DeFlores, K.C. Jones, A. Tokmakoff, *Acc. Chem. Res.* 41 (2008) 432.
- [32] H.J.C. Berendsen, D. van der Spoel, R. van Drunen, *Comp. Phys. Commun.* 95 (1995) 43.
- [33] W.F. van Gunsteren, et al., *Biomolecular Simulation: The GROMOS96 Manual and User Guide*, Hochschulverlag AG an der ETH Zürich, Zürich, 1996.
- [34] H.J.C. Berendsen, J.R. Grigera, T.P. Straatsma, *J. Phys. Chem.* 91 (1987) 6269.
- [35] T. Darden, D. York, L. Pedersen, *J. Chem. Phys.* 98 (1993) 10089.
- [36] D. Brown, J.H.R. Clarke, *Mol. Phys.* 51 (1984) 1243.
- [37] B.H. Besler, K.M. Merz Jr., P.A. Kollman, *J. Comput. Chem.* 11 (1990) 431.
- [38] S. Ataka, H. Takeuchi, M. Tasumi, *J. Mol. Struct.* 113 (1984) 147.
- [39] J. Kubelka, T.A. Keiderling, *J. Phys. Chem. A* 105 (2001) 10922.
- [40] N.G. Mirkin, S. Krimm, *J. Am. Chem. Soc.* 113 (1991) 9742.
- [41] S.K. Gregurick, G.M. Chaban, R.B. Gerber, *J. Phys. Chem. A* 106 (2002) 8696.
- [42] S. Song, S.A. Asher, S. Krimm, K.D. Shaw, *J. Am. Chem. Soc.* 113 (1991) 1155.